remote sensing

Article

Contributing Factors and Trend Prediction of Urban-Settled Population Distribution Based on Human Perception Measurement: A Study on Beijing, China

Junnan Qi [1,2], Qingyan Meng [1,2,3,*], Linlin Zhang [1,2,3], Xuemiao Wang [1,2], Jianfeng Gao [1,2], Linhai Jing [1] and Tamás Jancsó [4]

1 Aerospace Information Research Institute, Chinese Academy of Sciences, Beijing 100094, China
2 University of Chinese Academy of Sciences, Beijing 100049, China
3 Key Laboratory of Earth Observation of Hainan Province, Hainan Aerospace Information Research Institute, Sanya 572029, China
4 Alba Regia Technical Faculty, Obuda University, H-8000 Szekesfehervar, Hungary
* Correspondence: mengqy@radi.ac.cn

Abstract: Population migration, accompanied by urbanization, has led to an increase in the urban-settled population. However, quantitative studies on the distribution of urban-settled population, especially at fine scale, are limited. This study explored the relationship between characteristics of human perceived environment and the distribution of settled population, and proposed a quantitative method to predict the distribution trend of settled population. Through the semantic segmentation of street view images and accessibility calculation based on traffic isochrone and points-of-interest, we determined human perception factors. The influence of human perception factors was quantified using the geographic detector method, and the settlement intention index (SII) was constructed combining the analytic hierarchy process to predict the distribution trend of settled population. The results indicated the following. (1) Human perception was one of the important factors influencing the distribution of urban-settled population, and the cycling accessibility to traffic facilities was closely related to the distribution of settled population. (2) The accessibility and visibility of green space with low independent influence portrayed a strong enhancement on the interactive effect of other perception factors. (3) The SII mapping of Beijing showed that the SII was reliable. This study analyzes the role of human perception in shaping the environment, and provides reference for population-related urban planning problems.

Keywords: urban-settled population distribution; street-view images; points of interest; geographic detector; quantitative prediction index; block scale

Citation: Qi, J.; Meng, Q.; Zhang, L.; Wang, X.; Gao, J.; Jing, L.; Jancsó, T. Contributing Factors and Trend Prediction of Urban-Settled Population Distribution Based on Human Perception Measurement: A Study on Beijing, China. *Remote Sens.* **2022**, *14*, 3965. https://doi.org/10.3390/rs14163965

Academic Editors: Hua Liu, Qihao Weng, Umamaheshwaran Rajasekar and Li Zhang

Received: 10 June 2022
Accepted: 3 August 2022
Published: 15 August 2022

1. Introduction

Since 2008, more than half of the world's population has been living in cities [1]. Notably, large-scale population migration, accompanied by urbanization, has resulted in tremendous pressure on the limited urban resources and environmental capacity. Compared to developed countries, generally, the developing countries have a higher urban population growth rate, as well as a higher rate of internal migration from rural to urban settlements [2]. Cities in China and other developing countries are facing serious problems related to urban planning, resource allocation, and disaster emergency management [3–5]. To prevent and solve the above-mentioned problems, previous studies combined geography, economics, sociology, and other disciplines to predict urban population distribution [6]. At present, in multi-dimensional interdisciplinary studies, there is still a lack of quantitative research on the distribution of urban-settled population.

The SDG11 (Sustainable Development Goal 11) proposed in the international sustainable development policy of the 2030 Agenda is to make cities and human settlements inclusive, safe, resilient, and sustainable [7]. The settled population refers to the population with local registered residence and long-term residence. Settled population distribution data is necessary for the evaluation of indicators such as SDG11.3 (inclusive and sustainable urbanization and human settlement planning), SDG11.5 (reduce deaths and economic losses from disasters) and SDG11.7 (universal access to safe and inclusive green spaces). With the participation of satellite image products such as night light and land cover, the population grid data produced by machine learning methods such as random forest has been widely adopted [8]. Well-known population datasets such as LandScan have become the main population data sources for indicators evaluation of SDG11 due to their wide coverage and convenient acquisition [9]. However, the focus of current spatial population distribution studies has mainly been the total population, without considering the distinction between settled and floating populations. Moreover, most population maps use grid cells, thereby not accounting for irregularly shaped block cells, which are also inhabited [10–12].

Data on settled populations are mostly acquired through manual surveys, and such data cannot support spatial continuity and are difficult to obtain in a short time. Additionally, most existing studies on settled population distribution related to urban environment are based on census data. Due to privacy protection or unclear boundaries of geographical units, census data tend to summarize the population data only in a large area [13]. With the improvement in the accuracy of studies on the urban environment, a block is used as a representative of fine research unit in urban landscape and planning [14–16]. As a land unit having relatively homogeneous social and economic functions divided by road network, an urban block can aptly be considered the basic constituent unit of an urban structure and an important division unit that represents human activities in an area [17]. However, studies on the spatial distribution of settled population at block scale are limited.

The characteristics of urban environment have a profound influence on the priority of settlement choices and the stability of settlement [6]. Peoples' perceptions of urban environment, such as aesthetics, accessibility, and convenience, are closely related to their behavior [18,19]. Most existing studies on population settlement conducted to analyze peoples' preference to settle in an urban environment are based on questionnaire survey data [20–23]. The increase in the types of geospatial data and the development of processing technology have greatly enriched the methods that enable us to describe the characteristics of urban environment from a human perspective. At present, the urban environmental characteristics determined by population settlement studies can be summarized into two categories: the visual perception of public space and the spatial perception of urban facilities [21], which are detailed below:

(1) Urban public spaces include streets, squares, and other open spaces. Streets are the main places for urban peoples' daily activities and its landscape characteristics determine peoples' visual perceptions of the urban environment [6]. Meyer et al. (1994) [24] analyzed 100 cities around the world and indicated that the proper management of streets plays a key role in urban prosperity, in terms of the infrastructure, quality of life, equity, and inclusion. Due to limited data acquisition in the past, the existing studies on street visual perception are mainly based on field investigations [25]. As major mapping companies, such as Google, Baidu, and Tencent, collect street-view data using their mobile vehicles and make the data public, a large range of street landscape information can be obtained in batches through computer-vision algorithms. Some scholars conclude that the visual quality of streets is closely related to peoples' behavior and willingness to settle down [26,27]. However, there is no consensus on the methods to objectively and accurately measure peoples' visual perceptions of urban environments.

(2) Accessibility is the ability of people to overcome spatial barriers to access facilities [28] and has been regarded as an important factor that affects peoples' willingness to settle down [29–31]. Studies on the settlement areas of different populations indicate that almost all people prefer to live in places that offer better accessibility to education, health care, office, and transportation facilities [32], with the influence of office facilities being

the most obvious factor [33]. Due to the limitation of traditional data sources, accessibility measures are generally based on static plane spaces [34–36]. To reflect peoples' spatial perceptions of urban facilities accurately, it is important to consider the efficiency of road traffic, different transportation modes, and to have comprehensive information on road conditions [37]. The online location data platform provides a simple and feasible solution to the above problems. However, the most optimal method to reasonably combine network services with accessibility measurement methods remains an unresolved problem.

To solve the problem of insufficient quantitative research on the distribution of urban-settled population, in this study, we provided a novel view of study from the human perception of the urban environment. Based on the characteristic of human perceived urban environment, we analyzed the contributing factors of the distribution of settled population and constructed a quantitative distribution trend index. To the best of our knowledge, our work may be one of the first studies to use human-perceived characteristics of the urban environment to explore its influence on the distribution of settled populations and to establish a quantitative index. In addition, we used the online location data platform to improve the calculation method of accessibility.

This paper is organized as follows. Section 2 introduces the study area and data sources. Section 3 introduces the methods of establishing perception factors and the methods used for influence analysis and prediction index construction. Sections 4–6 present the results, discussion, and conclusions of the study. The flowchart of this study is shown in Figure 1.

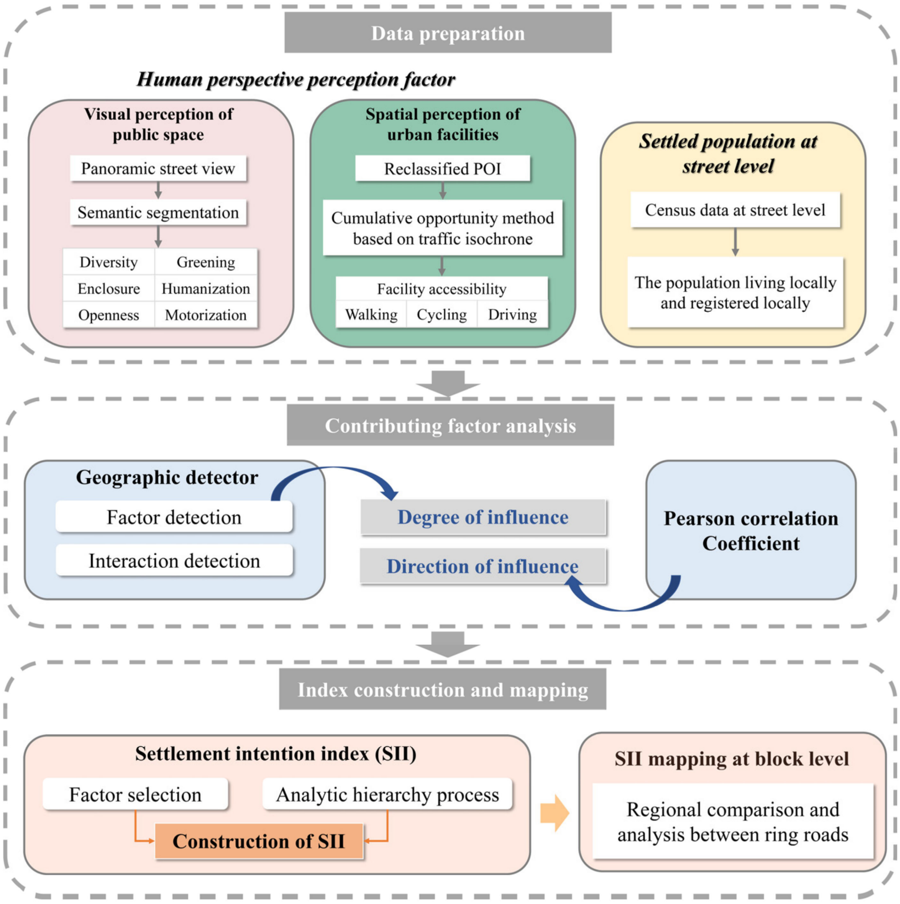

Figure 1. Flowchart of this study.

The objectives of this study were to: (1) comprehensively describe the characteristics of human perceptions of the urban environment, especially spatial and visual perceptions, and improve the computing power and accuracy of human perception factors through semantic segmentation and online location data platform; (2) analyze the independent and interactive influence of the characteristic of the human perception of urban environment on the distribution of settled population by using the geographic detector method; and (3) establish the settlement intention index (SII), using the analytic hierarchy process (AHP), based on the influence of human perception factors, and complete index mapping at block scale.

2. Materials

2.1. Study Area

Beijing is the capital of the People's Republic of China and the political, economic and cultural center of China; notably, it is also one of the most popular cities to settle down. [38]. We selected the fifth ring road in Beijing (which is the urban area of Beijing) as our study area (Figure 2). The study area occupied less than 5% of the total area of Beijing; however, 49% of the resident population of Beijing was distributed in this area (in 2015).

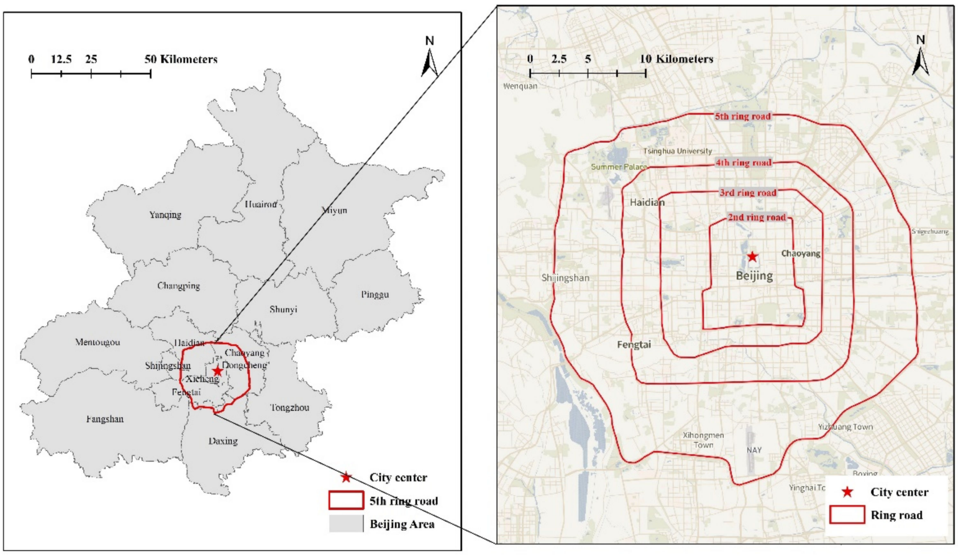

Figure 2. Map of the study area (fifth ring road) in Beijing, which covers the urban area of the city.

2.2. Data Description and Preprocessing

The land units used in this study included the street and block units. According to the data from the administrative division, there were 118 street units distributed in the study area. To ensure the accuracy of the statistical data, we considered only 114 street units, because four were mainly distributed outside the fifth ring road. Based on the urban plot data by Gong et al. [39], we selected 4280 plots over 300 m^2 distributed in the study area as the block units for this study. Notably, we used the following six data sets.

2.2.1. Street-View Images (SVI)

Panoramic SVIs are 360-degree pictures generated from eight original pictures captured by cameras on moving vehicles. Our collection of panoramic SVI was based on Baidu Map (https://map.baidu.com/, accessed on 23 January 2022). We used Baidu Map to obtain road network data in the study area, set sampling points (The endpoints at both ends of each road and 200-m interval points along road), and obtain images from these points (Figure 3a). A total of 120,953 images were collected from September to November, 2021. However, the process of merging planar images captured by horizontal cameras to form panoramic images can cause serious distortion at the top and bottom parts of the panorama images, along with slight distortion at the central part of the pitch angle (vertical angle) of $\pm 30°$ [40]. The bottom parts of the Baidu SVI (panorama) included the body of moving vehicles; therefore, we cut and retained one third of the vertical center part of the image for subsequent study (Figure 3b). To measure the visual closure of the street, Yin and

Wang also cropped the central part of the panoramic image in their study and indicated that the cropped image was more in line with the real field of view of pedestrians [41].

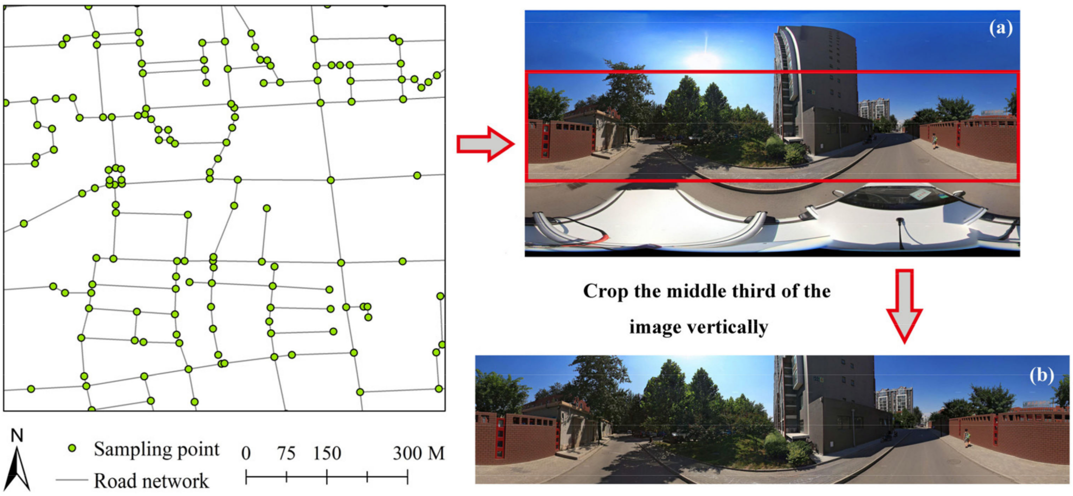

Figure 3. (**a**) Original street view images (SVIs) (panorama), (**b**) cropped SVIs.

2.2.2. Points of Interest (POI)

POI data can provide accurate geographic locations and detailed attribute information for urban facilities. In this study, we obtained the POI data of 666,144 facilities of different types distributed in the urban center of Beijing and its adjacent 12 administrative districts from AMAP (https://www.amap.com, accessed on 27 January 2022). The POI data included schools, restaurants, shopping malls, parking lots, parks, companies, and almost all physical facilities that people used on a daily basis. After deleting the incomplete and repeated records, we sorted the data into six categories, according to peoples' travel purposes: office, traffic, commerce, residence, scientific education and health, and green space and square.

2.2.3. Night-Time Light (NTL) Satellite Images

In this study, we used the monthly National Polar-Orbiting Partnership- Visible and Infrared Imager/Radiometer Suite (NPP-VIIRS) NTL data acquired from the National Aeronautics and Space Administration (NASA) in 2020, with a spatial resolution of 500 m. Notably, we used the data to perform annual image synthesis, re-projection, resampling, and clipping. In addition, we performed denoising to remove auroras, fires, and other transient light sources, as well as the background noise.

2.2.4. Density of the Settled Population (DSP)

The data of settled population used in this study were acquired from the sixth Beijing population census undertaken by the National Bureau of Statistics, which was the updated population data available at street scale. Notably, the census, designed and conducted by the state, is the most reliable population data in China. In this study, the census result type of "living locally, registered locally" were used to represent the spatial distribution of settled population. We calculated the ratio of this data for the corresponding street area to obtain the density of the settled population (DSP) at the street scale.

3. Methods

The methodology applied in this study can be roughly divided into four parts: (1) Perceptual information extraction: this step included the extraction of peoples' visual perceptual information of public spaces through the semantic segmentation of SVIs, and the extraction of peoples' spatial perceptual information of urban facilities by the cumulative opportunity method based on the isochrone application programming interface

(API). (2) Establishment of perception factors: this step was based on the types of extracted information and the characteristics of the urban environment; we sorted out and integrated the perceptual information to determine the human perception factors. (3) Contributing factor analysis: this step included the use of the geographic detector method to analyze the independent and interactive influences of each perception factor on the DSP. (4) Construction of distribution trend prediction index: this step was based on the influence of different perception factors on the DSP; we selected the index and used the AHP to build the index calculation model.

3.1. Perceptual Information Extraction

3.1.1. Semantic Segmentation

The SVIs reflect peoples' real visual perception of urban public spaces. To quantify this perception, we used the semantic segmentation to extract various elements in the SVIs. Semantic segmentation is a typical computer vision problem, which involves taking some original data (such as planar images) as input and converting them into masks with highlighted regions of interest. Compared with traditional segmentation algorithms, semantic segmentation automatically learns features from a large number of training data, which improved the segmentation accuracy and efficiency greatly. It enabled us to locate specific objects in an image and classify the image pixels into a specific category (from a series of discrete categories that describe the image). Semantic segmentation models commonly used in street view images include RefineNet, PSPNet, ResNet-38, DeepLab-v3, etc., of which DeepLab-v3 shows excellent performance on the cityscape test set [42]. DeepLab-v3 model has obvious improvement over the previous version of DeepLab, and has achieved performance equivalent to other advanced models. Therefore, we used DeepLab-v3 model for semantic segmentation of street view images. The model proposes the Atrous Spatial Pyramid Pooling (ASPP) module to mine the convolutional features of different scales, as well as the image layer features that encode global content information to improve the segmentation performance.

We used the Cityscape dataset to train the DeepLab-v3 model. The Cityscape dataset is a large dataset that can enhance the visual understanding of complex urban street scenes [43], including 19 types of urban street scenes, namely, road, side-walk, building, wall, fence, pole, traffic light, traffic sign, vegetation, terrain, sky, person, rider, car, truck, bus, train, motorcycle, and bicycle. The labeled data set is shown in Figure 4. To ensure the validity of the results, we removed the segmentation results that had unlabeled regions $\geq$30%. Finally, the scene element information of 116,865 street images were obtained.

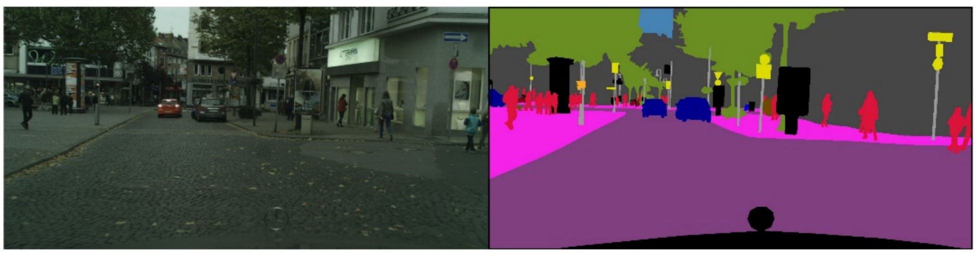

Figure 4. Test sample of Cityscape dataset (**left**: original image, **right**: labeled image).

3.1.2. Cumulative Opportunity Method Based on Traffic Isochrone

The isochrone API provided by Mapbox (http://mapbox.com, accessed on 27 January 2022) can calculate the reachable area from a certain location in the mode of walking, cycling, and driving within a specified time as the contour line of a surface or a line in vector format (Figure 5). The data obtained are known as the traffic isochrone. In general, isochrone API designs different travel paths for different modes of travel: walkways and trails are preferred for walking; streets with bike lanes are preferred for cycling; and highways are preferred for driving. Notably, traffic conditions use the real-time traffic speeds directly observed 15 min before generation. Some countries and regions, such as China, cannot provide real-time traffic conditions and use typical traffic speeds that reflect the normal traffic conditions in a historical week.

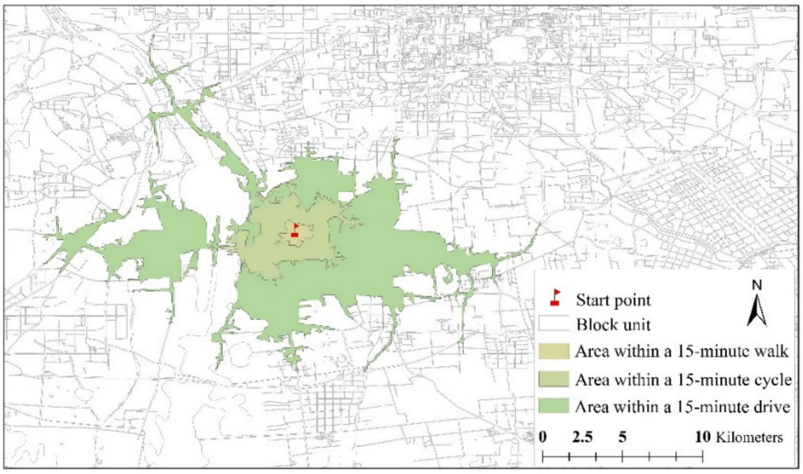

Figure 5. Example of isochrone data obtained using the isochrone API.

Based on different objectives, scholars have proposed different methods to measure accessibility [36]. The cumulative opportunity method considers the number of access opportunities within the range of a certain transportation cost (distance, time, and cost) as an index of accessibility. The higher the number of opportunities, the higher the level of accessibility. Moreover, in this method, isochrone API can simplify the calculation process of transportation cost. The vector range of traffic isochrone, combined with the spatial position information of POI, can be used to calculate accessibility more comprehensively, while considering the spatiotemporal distance.

The concept of "15-min community living circle" was proposed in Shanghai's 2040 Master Plan [44]. In this study, we adopted this concept. Notably, we considered 15 min as the time limit of the traffic isochrone circle, to determine the reachable area by walking, cycling, and driving, individually. Based on the classified POI data, the number of various facilities within the travel range was calculated to represent the accessibility of various facilities for different travel modes. To avoid the interference of road distribution within the study unit in the calculation of accessibility, we extracted the centroid of each block as the starting point.

3.2. Establishment of Perception Factors

In this study, we determined 25 perception factors from two aspects: peoples' spatial and visual perception of the urban environment (Table 1).

3.2.1. Visual Perception Factors of Public Space

Human visual perception of the scene includes a variety of information, such as the element types, texture features, and color saturation. Considering the operability of automatic calculation and measurement, we established the visual perception factors for the direct features of the scene, namely the proportion and diversity of elements. Example of segmentation and visual perception factor values of public space are shown in Figure 6. The original image (SVI) is shown at the top, and the segmented image is shown below it. In the segmented image, we used different colors to represent different visual elements in the public space. At the bottom, we listed the values of various visual perception factors calculated based on the SVI. The description of each factor is shown in Table 1. Taking the SVG value of 15.02 as an example, it represents the visibility of greening observed from the SVI sampling point is 15.02. The higher the calculated values of the visual perception factors, the stronger the human perception of the relevant landscape elements in public space.

Table 1. Basic information of human perception factors analyzed in this study.

Type	Metrics	Acronym	Description
Visual perception factors of public spaces	Street visual greening	SVG	$\mathrm{SVG} = P_{vegatation}$
	Street visual sky openness	SVS	$\mathrm{SVS} = P_{sky}$
	Street visual enclosure	SVE	$\mathrm{SVE} = P_{building} + P_{pole} + P_{fence} + P_{wall}$
	Street visual motorization	SVM	$Motorization = P_{road} + P_{traffic\ light} + P_{traffic\ sign} + P_{car} + P_{bus} + P_{trunk} + P_{motorcycle} + P_{train}$
	Street visual humanization	SVH	$Humanization = P_{person} + P_{sideway} + P_{rider} + P_{bicycle}$
	Shannon's diversity index	SHDI	$\mathrm{SHDI} = -\sum_{i=1}^{m} P_i * \ln P_i$
	Simpson's Diversity Index	SIDI	$\mathrm{SIDI} = 1 - \sum_{i=1}^{m} {P_i}^2$
Spatial perception factors of urban facilities	Walking accessibility to office facilities	W-O	Number of office facilities within a 15-min walk
	Walking accessibility to traffic facilities	W-T	Number of traffic facilities within a 15-min walk
	Walking accessibility to commercial facilities	W-C	Number of commercial facilities within a 15-min walk
	Walking accessibility to residential facilities	W-R	Number of residential facilities within a 15-min walk
	Walking accessibility to science education and health facilities	W-SH	Number of science education and health facilities within a 15-min walk
	Walking accessibility to green space and square facilities	W-G	Number of green space and square facilities within a 15-min walk
	Cycling accessibility to office facilities	C-O	Number of office facilities within a 15-min cycle
	Cycling accessibility to traffic facilities	C-T	Number of traffic facilities within a 15-min cycle
	Cycling accessibility to commercial facilities	C-C	Number of commercial facilities within a 15-min cycle
	Cycling accessibility to residential facilities	C-R	Number of residential facilities within a 15-min cycle
	Cycling accessibility to science education and health facilities	C-SH	Number of science education and health facilities within a 15-min cycle
	Cycling accessibility to green space and square facilities	C-G	Number of green space and square facilities within a 15-min cycle
	Driving accessibility to office facilities	D-O	Number of office facilities within a 15-min drive
	Driving accessibility to traffic facilities	D-T	Number of traffic facilities within a 15-min drive
	Driving accessibility to commercial facilities	D-C	Number of commercial facilities within a 15-min drive
	Driving accessibility to residential facilities	D-R	Number of residential facilities within a 15-min drive
	Driving accessibility to science education and health facilities	D-SH	Number of science education and health facilities within a 15-min drive
	Driving accessibility to green space and square facilities	D-G	Number of green space and square facilities within a 15-min drive

P_i stands for the proportion of the landscape occupied by element type (class) I; m stands for the total number.

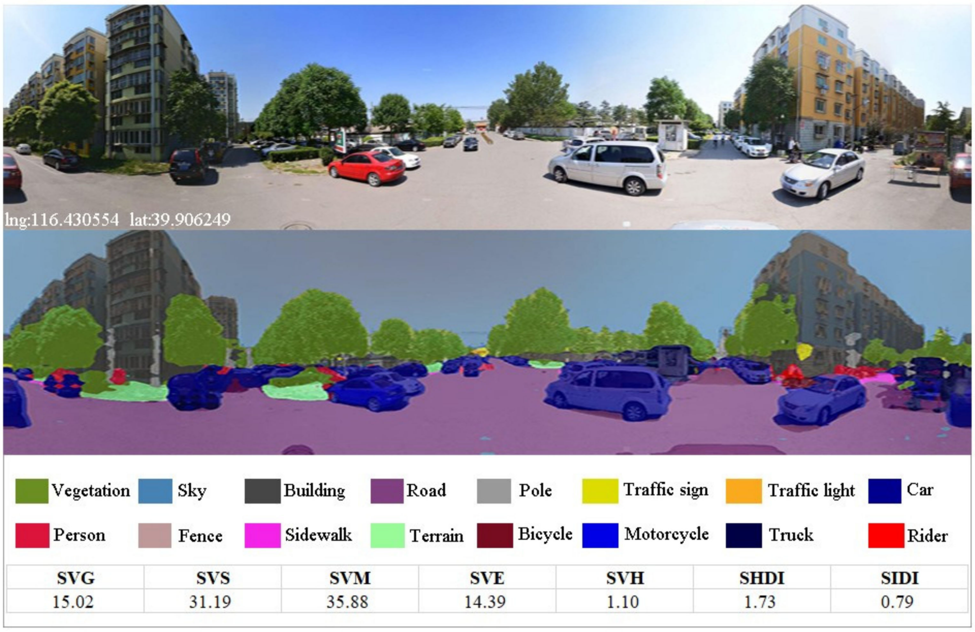

Figure 6. Example of SVI semantic segmentation results and the values of public space visual perception factors calculated based on the SVI. Abbreviations: street visual greening (SVG), street visual sky openness (SVS), street visual enclosure (SVE), street visual motorization (SVM), street visual humanization (SVH), Shannon's diversity index (SHDI), Simpson's diversity index (SIDI).

1. Proportion of elements:

Similar to the top-down land cover information obtained from remote sensing images, the proportions of elements in SVIs provide more detailed land cover information from the human perspective. Based on the definition of greening, openness, and closeness in SVIs proposed by Tang and Long [45], we designed five visual perception factors, namely street visual greening (SVG), street visual sky openness (SVS), street visual enclosure (SVE), street visual motorization (SVM), and street visual humanization (SVH), which are explained in detail below.

- Street visual greening (SVG): The greening elements include visible information about various types of vegetation. Greening at the urban street level makes a significant contribution to the attractiveness and walkability of residential streets [46]. Green streets are often the main places for people to take a walk, jog, and partake in sports activities [47]. Therefore, greening is one of the important factors of urban ecological environment construction.
- Street visual sky openness (SVS) and street visual enclosure (SVE): The visual perception of the degree of sky openness and closure of urban public spaces reflects the spaciousness of urban roads and the height, density, and continuity of buildings. These are all important factors that affect the comfort and livability of the residents [48,49]. Notably, these two factors describe the characteristics of the elements associated with the building environment.
- Street visual motorization (SVM) and street visual humanization (SVH): SVM represent the suitability of the street scene for automobile traffic and reflects the density of motor vehicle traffic at that time. SVH reflects the element information related to walking and cycling, that is, the humanization degree of the street environment for peoples' activities. Therefore, these two factors describe the characteristics of elements related to peoples' traveling activities.

2. Diversity of elements:

Landscape diversity, as described in landscape ecology, refers to the variations in and complexity of landscape elements in a given study area. In this study, we used Shannon's diversity index (SHDI) and Simpson's diversity index (SIDI) in landscape ecology to quantitatively describe the element diversity across the street scenes [50]. Notably, SHDI is sensitive to rare elements, and the larger the value of the index, the more complex the landscape structure is and the more information it contains. Compared to SHDI, SIDI is less sensitive to rare element types, and its interpretation is more intuitive.

3.2.2. Spatial Perception Factors of Urban Facilities

Accessibility is the result of facility distribution and the traffic state. Based on the abovementioned accessibility calculation method, we calculated the accessibility for the three different travel modes for six types of POIs; the results were used to represent peoples' spatial perceptions of urban facilities.

The accessibility of different types of facilities affects peoples' behavior and lifestyle in different aspects. Notably, the spatial distribution of commercial facilities has an effective and lasting effect on the distribution of urban population on rest days [51]. Generally, the populations in areas having a dense distribution of parks and leisure attractions portray a higher frequency of daily leisure activities [52]. Additionally, the accessibility of work facilities reflects, to some extent, the distribution of social classes and ethnic groups living in the area [33,53].

Several previous studies analyzed the accessibility of a single mode of transportation, but only few studies considered the accessibility of multiple modes of transportation comprehensively and conducted a comparative analysis. Yan indicated that the accessibility of walking, public transport, and driving had different influence on peoples' settlement choices [54]. Notably, to consider different transportation modes in the establishment of spatial perception factors, it is important for the comprehensiveness of spatial perception factors.

3.3. Geographic Detector Method

The geographic detector method is used to statistically detect and utilize spatial heterogeneity in geographical phenomena; this information can be used to reveal the explanatory factors of the phenomena and analyze the interactions between different variables [55]. Geographical detectors have been widely used in environmental studies and perform efficiently [26,56,57].

3.3.1. Factor Detection

In factor detection, we use q values to measure the interpretation degree of perception factors with respect to the spatial heterogeneity of the DSP, which can be expressed as follows:

$$\mathrm{q} = 1 - \frac{\sum_{h=1}^{L} N_h \sigma_h^2}{N\sigma^2} = 1 - \frac{\mathrm{SSW}}{\mathrm{SST}}, \tag{1}$$

$$\mathrm{SSW} = \sum_{h=1}^{L} N_h \sigma_h^2, \tag{2}$$

$$\mathrm{SST} = N\sigma^2, \tag{3}$$

where dependent variable (Y) and independent variable (X) constitute the strata having a total number L; N_h and σ_h^2 represent the number of units in h layer and the variance of Y value in h layer, respectively. Moreover, N and σ^2 represent the number of units and the variance of Y value, respectively, for the entire region. Strata are generally generated by the discretization of X. Notably, SSW represents the sum of the variances in the layer, and SST represents the sum of the variances for the entire region. The smaller the ratio, the more obvious the spatial heterogeneity of Y. The q values range from 0 to 1. The explanatory strength can be quantified as $100 \times \mathrm{q}\%$.

3.3.2. Interaction Detection

Interaction detection is used to identify the interaction between different perception factors. It can evaluate whether the joint action of factors will increase or decrease the explanatory power of Y and also, determine if the effects of these two factors on Y are independent of each other.

The evaluation method for interaction detection is explained below. First, the q values of X_1 and X_2 for Y are calculated, respectively. Thereafter, the stratum of X_1 is intersected with the stratum of X_2 to form a new stratum, and the q value of $X_1 \cap X_2$ to Y is calculated; qX_1, q(X_2) and q$(X_1 \cap X_2)$ were compared and classified according to Table 2.

Table 2. Interaction classification criteria.

Criterion	Interaction
$q(X_1 \cap X_2) < Min(q(X_1), q(X_2))$	Weaken (nonlinear)
$Min(q(X_1), q(X_2)) < q(X_1 \cap X_2) < Max(q(X_1), q(X_1))$	Uni-weaken(nonlinear)
$q(X_1 \cap X_2) > Max(q(X_1), q(X_1))$	Bi-enhance
$q(X_1 \cap X_2) = qX_1 + q(X_2)$	Independent
$q(X_1 \cap X_2) > qX_1 + q(X_2)$	Enhance (nonlinear)

3.4. *Analytic Hierarchy Process (AHP)*

The analytic hierarchy process (AHP) decomposes the problem into different component factors according to the nature of the problem and the overall goal to be achieved, and aggregates and combines the factors at different levels according to the interrelated influence and membership relationship between the factors to form a multi-level analysis structure model. Thus, the problem is finally attributed to the determination of the relatively important weight of the lowest level (schemes and measures for decision-making) relative to the highest level (overall goal) or the arrangement of the relative advantages and disadvantages. The AHP is a multidimensional criterion decision-making method for the quantitative analysis of fuzzy and complex problems [56,57]. Notably, the AHP structures the problems and forms a hierarchical system of goals, criteria, and indicators [58]. At present, the AHP has been widely used in the construction of quantitative models in various fields [59–63]. The main steps of determining the indicators' weight using the AHP are explained below:

1. Establishing discriminant matrix

Generally, the judgment matrix is established according to the contribution of each factor to the upper level and the corresponding significance of the scale of the judgment matrix. The discriminant matrix is shown in Equation (4) below.

$$X = \begin{bmatrix} x_{11} & x_{12} & \cdots & x_{1j} \\ x_{21} & x_{22} & \cdots & x_{2j} \\ \vdots & & & \vdots \\ x_{i1} & x_{i2} & \cdots & x_{ij} \end{bmatrix}, \tag{4}$$

where X_i, X_j $(i, j = 1, 2, 3, \ldots\ldots n)$ represents the factor of item i or item j, and n represents the total number of indicators. X_{ij} indicates the importance of X_i, compared to X_j. Moreover, we used the "nine scale" method proposed by Saaty (1980), to quantify the relative importance of each indicator (Table 3).

Table 3. Scale meaning of "nine scale" method.

Scale	Meaning
1	Compared with *j*, *i* and *j* have the same influence
3	Compared with *j*, *i* has a slightly stronger influence
5	Compared with *j*, *i* has a obviously stronger influence
7	Compared with *j*, *i* has an especially stronger influence
9	Compared with *j*, *i* has a extremely stronger influence
2, 4, 6, 8	The intermediate situation of the above two adjacent judgment results
1, 1/2, ... , 1/9	The influence ratio of *i* and *j* is contrary to the above description

2. Measuring the consistency of the matrix

In this process, the relevant indicators include the consistency index (*CI*), random consistency index (*RI*), and consistency ratio (*CR*). Generally, when $CR < 0.1$, the weight distribution of the discrimination matrix was reasonable and passed the consistency test.

$$CI = \frac{\lambda_{max} - n}{n - 1}, \tag{5}$$

$$CR = \frac{CI}{RI}, \tag{6}$$

where λ is the eigenvector, which is calculated by the square root method. Notably, RI increased with increase in the order of judgment matrix.

3. Calculation of indicator' weight

When the consistency of the indicators met the requirements, the eigenvectors corresponding to each indicator were calculated according to the maximum eigenvalues of the matrix. These values were then, standardized and transformed into weight vectors (the sum of each component of the feature vector was 1), to calculate the weight corresponding to the indicators.

4. Results

4.1. Analysis of Contributing Factors, Based on the Geographic Detector Method

Our results were based on the factor values at street scale. Due to the limitation of the accuracy of the settled population data, we use the average of the perception factors of each block unit in the street unit to represent the average level of people's perception of the urban environment in the street unit. Factor calculation was carried out at block scale, and the street scale factor the average value of its internal block factors. Generally, the NTL data has been proved to be an important parameter that reflect urban construction, economic activities, and population distribution [64]. When using the factor detection of geographical detector, the relative importance of different factors is judged by comparing the q value. Notably, the single q value obtained by factor detection cannot directly represent the influence degree of this factor. To objectively prove the importance of each perception factor on the spatial distribution of the settled population in Beijing, we added the mean value of the NTL data of each street unit as the reference factor. The following results were obtained using geographic detectors.

4.1.1. Relative Importance of Perception Factors

The results of factor detection are shown in Figure 7a. In addition to SIDI, SVM, and SVG, the q values of other 22 factors, whose q values were higher than the NTL data, were significant at 0.001; this proved that these 22 perception factors had important influence on the DSP.

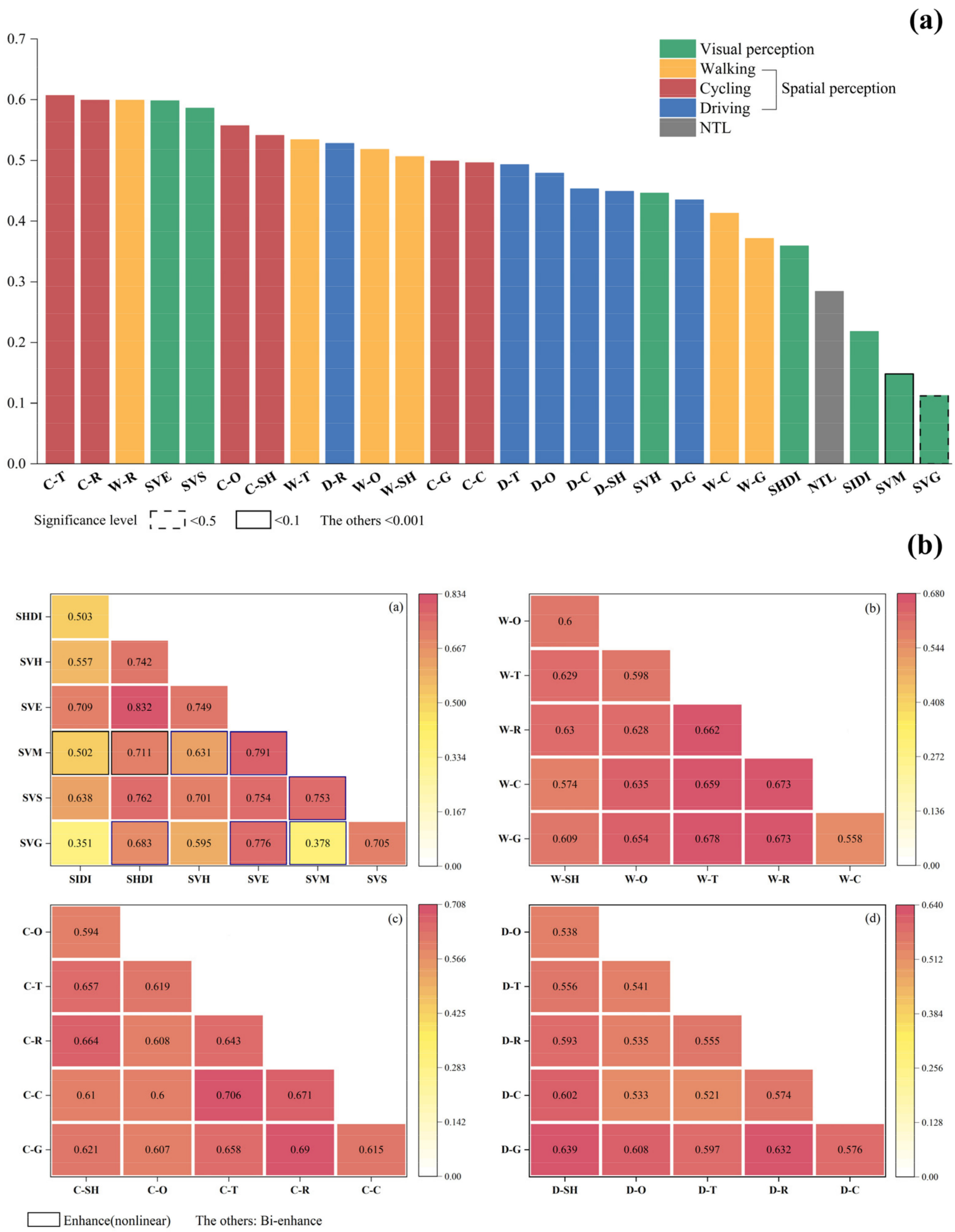

Figure 7. (**a**) Influence of human perception factors on the density of the settled population (DSP), sorted from high to low and (**b**) interactions between human perception factors and DSP.

Figure 8 portrays the top five perception factors of q value and the spatial distribution of the DSP, including three spatial perception factors and two visual perception factors. Notably, the difference in the q values of the factors was very small, which indicated that both types of perception factors had a significant influence on the DSP.

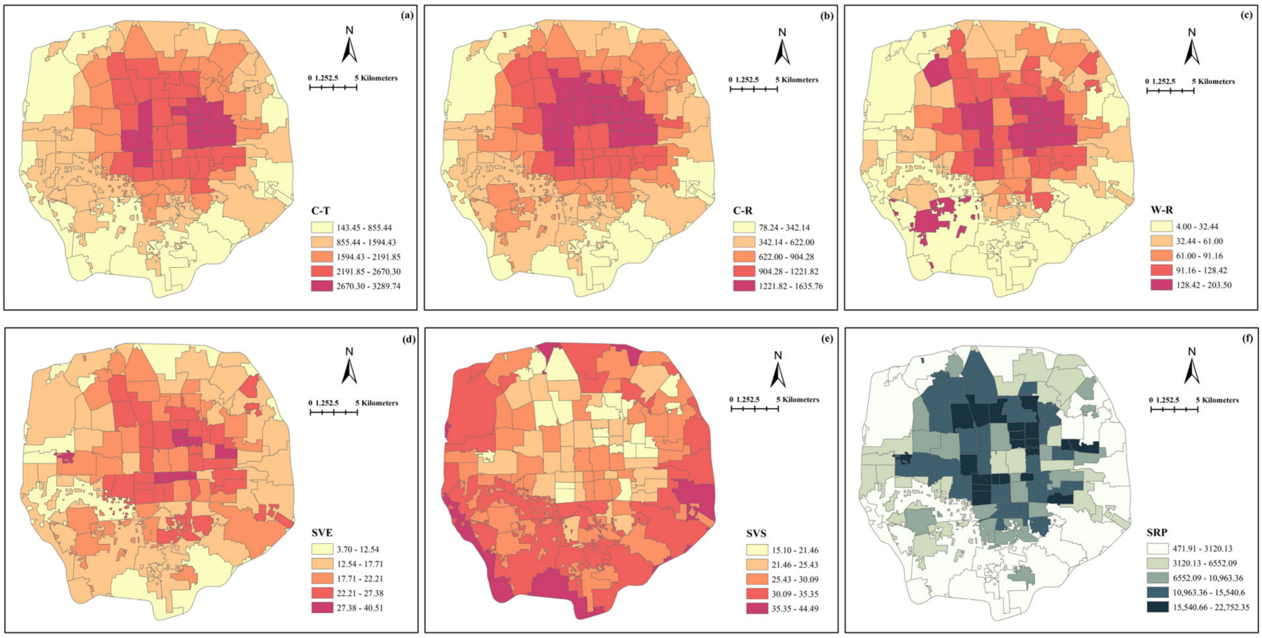

Figure 8. The spatial distribution of the top five perception factors of q value and DSP. (**a**) C-T (**b**) C-R (**c**) W-R (**d**) -SVE (**e**) SVS (**f**) DSP.

The order of relative importance of the visual perception factors in public spaces to the DSP was SVE > SVS > SVH > SHDI > SIDI > SVM > SVG. Notably, the SVE and SVS affected the DSP at a relatively high level, indicating that the visual perception factors related to the building environment had a great influence on the DSP. The q value of SVH was much higher than that of SVM, indicating that more people preferred to settle down in areas that were suitable for walking and cycling activities than those suitable for motor vehicles. Moreover, the influence of SHDI was low, but had a greater effect that the NTL data; notably, the value of SHDI was higher than that of SIDI, indicating that the emergence of rare elements in visual perception was more important than intuitive diversity. Gong et al. portrayed that the richness of element types often implied more complete local urban functions [65]. To our surprise, the greening construction of public spaces did not have a significant influence on the DSP. In addition, we used factor detection to obtain the interpretation rate of DSP for the spatial heterogeneity of visual perception factors in public space (Table 4). The influence of DSP on the environmental characteristics of public space influenced the relative importance of visual perception factors to a certain extent. However, it can be seen from Table 4 that street landscape plays a more obvious role in promoting DSP. Therefore, the relative importance of visual perception factors still follows Figure 7a.

Table 4. The factor detector results of DSP on visual perception factors in public space.

SVG	SVS	SVM	SVE	SVH	SHDI	SIDI
/	0.38 ***	/	0.42 ***	0.29 ***	/	/

*** denotes $p < 0.001$ in the significance test.

In this study, the relative importance of spatial perception factors of urban facilities to the DSP was compared from the perspective of travel mode and facility type: (1) For different travel modes, the accessibility to residential, traffic, and office facilities in the three travel modes had the highest effects on the DSP. The cycling and driving accessibility to green space and square facilities had the least influence on the DSP. Compared with the other two travel modes, the driving accessibility of commercial facilities had a greater influence on the DSP. (2) For different types of facilities, among the three travel modes, the cycling accessibility to various facilities had the greatest influence. The driving accessibility to traffic, residential, office, and education and health facilities had the least influence on the DSP. The cycling accessibility to commercial facilities, green spaces, and square facilities had the least influence on the DSP. Notably, the spatial perception factors related to green spaces and squares had minimal influence on the DSP, which was similar to the influence of the SVG.

4.1.2. Joint Influence of Perception Factors

Further, we divided the 25 perception factors into four groups, according to their types, and conducted an interaction detection analysis of the geographic detectors to determine the joint influence between the two factors, when the four groups of factors influenced the DSP (Figure 7b). We observed that, when the four groups of factors influenced the DSP, any two factors portrayed two types of mutual enhancement, namely, double factor enhancement and nonlinear enhancement. This indicated that the joint influence of any two perception factors strengthened the explanatory power of the DSP; this also indicated that the DSP was the result of the joint influence between the factors. The steps applied for interaction detection for the visual and spatial perception factors are explained in detail below:

(1) Interaction detection of visual perception factors: Although the influence of the SVM and SVG on the DSP was not obvious, $q(SVG \cap SVM)$, $q(SVG \cap SHDI)$, $q(SVG \cap SVE)$ and the interaction between the SVM and other six factors portrayed nonlinear enhancement (the strongest type of enhanced interaction). This indicated that the influence of the SVM and SVG on the DSP was mainly reflected in their interaction with other factors. The q value of the joint influence of the SVE and other factors was higher than 0.7, with the maximum value being 0.832. The perception factors that had a significant influence on factor detection also portrayed a stronger explanatory power, when combined with other factors.

(2) Interaction detection of spatial perception factors: The mutual enhancement type between two factors in each group was two-factor enhancement, and when any two factors acted together, they had a similar explanatory power to DSP (0.521–0.706). In each group, the combinations having the strongest explanatory power of joint action were $q(W-T \cap W-G)$, $q(C-T \cap C-C)$, $q(D-SH \cap D-G)$. Notably, these three combinations contained the factors that portrayed the lowest degree of influence in each group. To our surprise, among all the driving perception factors, the two factors that had the lowest independent influence portrayed the highest explanatory power for the DSP.

4.2. Construction of Distribution Trend Prediction Index Based on Analytic Hierarchy Process (AHP)

To avoid the redundancy of the SII model, we screened the factors involved in the construction of the model, while ensuring rationality and comprehensiveness. Among all the visual perception factors of public spaces, we selected SVE, SVS, SVH, and SHDI, which had significant influences on the DSP. Among the spatial perception factors of urban facilities, we selected the factors that had the most significant influence on each type of facilities, namely C-T, C-R, C-O, C-SH, C-G, and C-C (these terminologies have been explained in Table 1). Therefore, a total of 10 factors were used for the construction of SII.

4.2.1. Analysis of Pearson Correlation Coefficient (PCC)

To further understand the correlation between each perception factor and the DSP, we drew the scatter diagram of each perception factor against the DSP and calculated the Pearson correlation coefficient (PCC) (Figure 9). Moreover, the scatter diagram portrayed a linear correlation between the 10 perception factors involved in the construction of the SII and the DSP. Notably, the SVS was negatively correlated with the DSP, whereas the other factors portrayed a positively correlation. According to PCC, the correlation between each factor and the DSP was significant, with the correlation coefficient between them being greater than 0.4, indicating that the relationship between each factor and the DSP was close. The absolute value of PCC between the C-T, C-R, and SVS factors and the DSP was greater than 0.7, indicating that the relationship between them was very close. The results of the correlation analysis portrayed that the selected factors were reasonable and could be used to construct the SII effectively. Simultaneously, the correlation direction between each factor and the DSP also provides guidance for the construction of the SII.

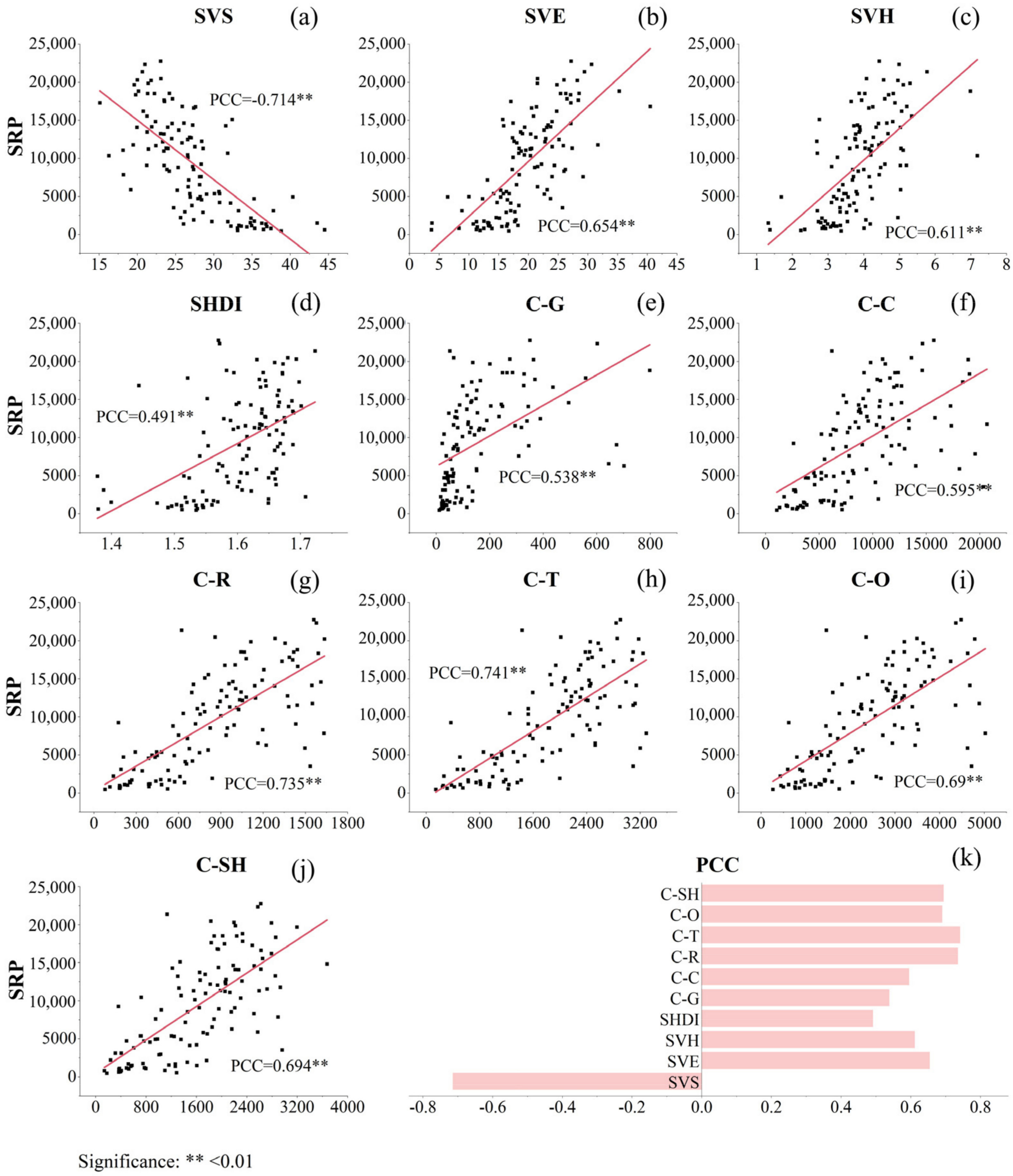

Figure 9. (**a**–**j**) Scatter diagram of human perception factors and the density of the settled population (DSP) (**k**) Pearson correlation coefficient (PCC) between human perception factors and the density of the settled population (DSP).

4.2.2. Index Calculation Model

According to the idea of the "nine scale" method and the results of factor detection in the geographic detector method, we determined the core principle for constructing a comparison matrix, using Equation (7), as follow:

$$X_{ij} = \begin{cases} 1 + \mathrm{int}\left(\frac{q_i - q_j}{0.1}\right), & q_i > q_j \\ \frac{1}{1+\mathrm{int}\left(\frac{q_j - q_i}{0.1}\right)}, & q_i < q_j \end{cases}, \tag{7}$$

where X_{ij} indicates the importance of X_i, compared to X_j, and q_i, q_j $(i, j = 1, 2, 3, \ldots\ldots n)$ represents the q value of item i or item j of factor detection.

The pairwise comparison matrix was obtained according to the abovementioned principle, as shown in Figure 10. The CR of the three matrices was less than 0.1 and passed the consistency test. Finally, the weight of each factor in the SII model was obtained using the AHP (Table 5). Combined with the results of the Pearson correlation analysis, the weight of the SVS factor was negative, whereas those of the other factors were positive. In summary, the SII calculation formula was constructed according to the steps described below.

$$\begin{aligned} \mathrm{SII} = {} & 0.1786{*}\mathrm{SVE} - 0.1786{*}\mathrm{SVS} + 0.0806{*}\mathrm{SVH} + 0.0659{*}\mathrm{SHDI} + 0.1028{*}\mathrm{C} - \mathrm{T} + 0.1028{*}\mathrm{C} - \mathrm{R} \\ & + 0.0819{*}\mathrm{C} - \mathrm{O} + 0.0819{*}\mathrm{C} - \mathrm{SH} + 0.0653{*}\mathrm{C} - \mathrm{G} + 0.0653{*}\mathrm{C} - \mathrm{C} \end{aligned} \tag{8}$$

CR=0.0000

A	B1	B2
B1	1	1
B2	1	1

CR=0.0077

B1	C1	C2	C3	C4
C1	1	1	2	3
C2	1	1	2	3
C3	1/2	1/2	1	1
C4	1/3	1/3	1	1

CR=0.0170

B2	C5	C6	C7	C8	C9	C10
C5	1	1	1	1	2	2
C6	1	1	1	1	2	2
C7	1	1	1	1	1	1
C8	1	1	1	1	1	1
C9	1/2	1/2	1	1	1	1
C10	1/2	1/2	1	1	1	1

Figure 10. Pairwise comparison matrix. (A) SII, (B1) visual perception factors of public space, (B2) spatial perception factors of urban facilities, (C1) SVE, (C2) SVS, (C3) SVH, (C4) SHDI, (C5) C-T, (C6) C-R, (C7) C-O, (C8) C-SH, (C9) C-G, (C10) C-C.

Table 5. Hierarchy and metric weight of settlement intention index (SII) model.

Target Layer	Rule Layer	Index Layer	Weight
Settlement intention index (SII)	Visual perception factor of public space	SVE	0.1768
		SVS	0.1768
		SVH	0.0806
		SHDI	0.0659
	Spatial perception factor of urban facilities	C-T	0.1028
		C-R	0.1028
		C-O	0.0819
		C-SH	0.0819
		C-G	0.0653
		C-C	0.0653

For abbreviations, please see Table 1.

For abbreviations, please see Table 1. Notably, to eliminate the influence of dimension, when calculating the SII, before input, all the perception factors were standardized to 0–1.

4.3. Settlement Intention Index (SII) Mapping at Block Scale

We used the SII calculation model to determine the distribution of the SII at block scale in the fifth ring road of Beijing. The SII values of each block within the fifth ring road in Beijing ranged from −0.11 to 0.55. To make the spatial distribution of SII values clearer, we used the natural breaks method to divide the blocks into eight categories according to the SII value (Figure 11a). The study area was divided into four areas, namely A, B, C, and D, by the ring line, from the center of the area to its periphery. Area A, also known as the Old City, are known as the central government functional area of Beijing. Areas A, B and C are known as the central districts of Beijing and have the most mature life support services. Area D is known as park district of Beijing. Large-scale urban greening and parks have been built in area D, and the supporting service facilities for life are insufficient compared with other areas. The distribution of the SII in each area is shown in Figure 11b. From the center of Beijing urban area to the fifth ring road, the SII portrayed an obvious decreasing trend, with the decline being most obvious in the south. SII values obviously varied with the urban planning and construction in different areas of the city. The more perfect the living supporting service of the block, the higher the value of SII. Similarly, the more inhospitable the neighborhood, the lower or even negative the SII. To further verify the calculation results of SII, we extracted the high-value (top 20%) and low-value (bottom 20%) areas of the SII, as shown in Figure 11c. Specifically, the SII value range of high value area is −0.11 to 0.02, and the SII value range of low value area is 0.42 to 0.55. The high value areas were concentrated in the north of Area A and the east and north of Area B. In terms of the administrative division, the high value areas of the SII involved the Dongcheng, Xicheng, Chaoyang, and Haidian districts, which were consistent with the development and construction level of the Beijing administrative region. The low value area of the SII was mainly distributed near the outer edge of Area B. The boundary of the fifth ring road was close to the suburbs, which consisted of industrial areas, airports, and scenic spots, where people did not prefer to, or could not, settle. The low value areas of the SII in areas A, B, and C mostly consisted of uninhabitable blocks, such as large parks and bare land, such as the Beihai, Yuyuantan, and Longtan parks and the bare land areas in the southwest of Area B. A few low SII-value areas portrayed an irregular "L" or "U" shape that had small distribution areas, mostly consisting of street shops and green belts. These results portrayed that the calculation results of the SII were reliable and consistent with general cognition.

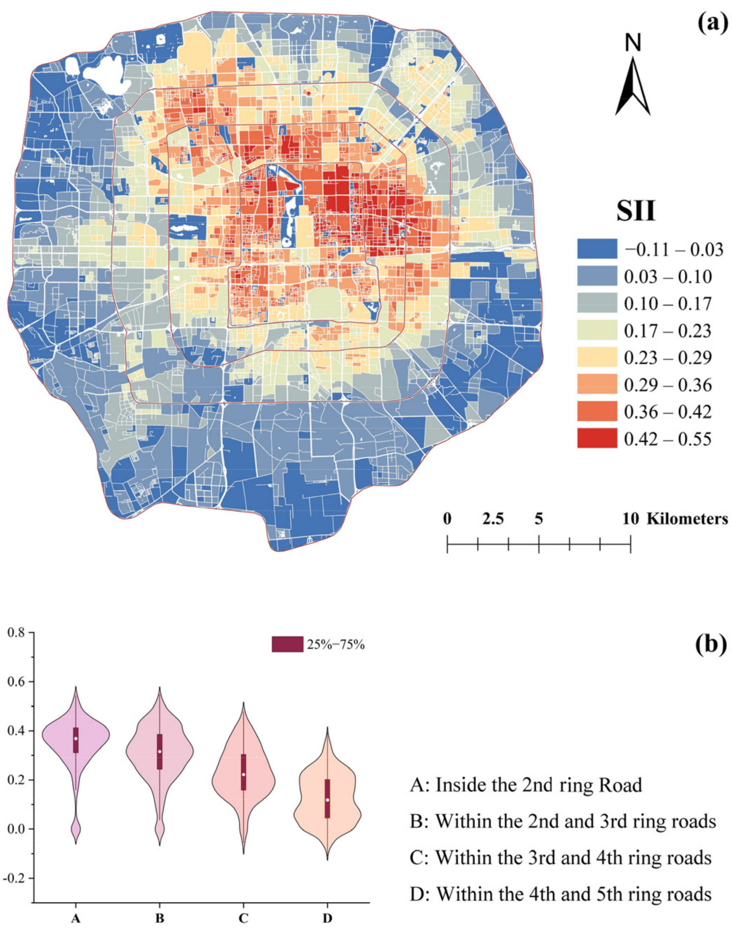

Figure 11. *Cont.*

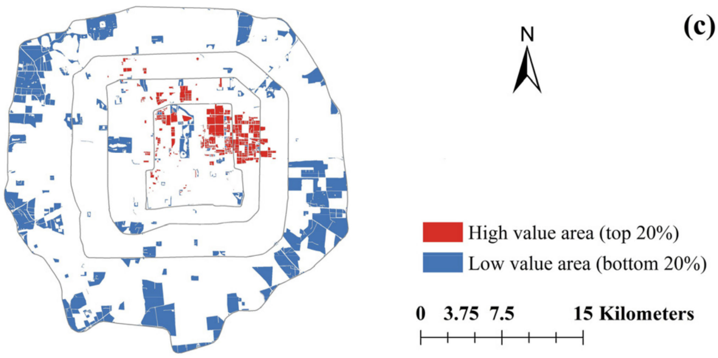

Figure 11. (**a**) Spatial distribution of settlement intention index (SII), (**b**) violin diagram of SII between ring roads, and (**c**) spatial distributions of high and low values of SII.

5. Discussion

5.1. Methodological Contributions

Previous studies analyzed the influence of urban environment and human perception on the settlement behavior of people, with only a few studies analyzing the characteristics of human perceived urban environment, to study the distribution of settled population. In this study, we used open-source data and automatic processing tools to make a fine and comprehensive description of the human perception of an urban environment. We used DeepLab-v3 and isochrone API to extend the use of SVIs and POI and enable the automatic large-scale quantitative extraction of human perceived information of urban environment. On the basis of previous studies, we established perception factors from the human perspective, while covering a variety of visual and spatial perception factors. Geographic detectors have been proved to be powerful tools. They can process different types of data flexibly, reveal the individual and interactive effects of various factors on the DSP, and serve as a foundation for the construction of the SII. The results of factor detection and PCC guided the establishment of the AHP judgment matrix and increased the reliability and objectivity of the SII, while skillfully avoiding the weight calculation error caused by strong subjectivity.

Notably, the SII values cannot represent the actual value of the spatial distribution of the settled population in an area. However, the SII is used to predict the relative distribution trend of settled population in the short term. Generally, the population in the same area is constantly changing [66]. The SII represents the trend of accumulation or loss of settled population in the current urban environment. It can also be used to evaluate the attractiveness of each block to the new urban-settled population and internal relocated population.

5.2. Potential Contributions

5.2.1. Relationship between Settlement Intention Index (SII) and Urban Land Use Categories

Using the map of essential urban land use categories in China (EULUC-China) drawn by Gong et al. [39], we summarized the distribution of the SII values for the land use types of each block (Figure 12a). According to the average value of SII, different land use types were sorted as: business office, administrative, medical, educational, sport and cultural, residential, commercial service, park and greenspace, industrial. Among them, the average value and distribution range of SII of administrative, medical, educational, sport and cultural were similar. The SII value of residential had the widest distribution range. The SII value distribution of industrial was significantly lower than that of other land use types.

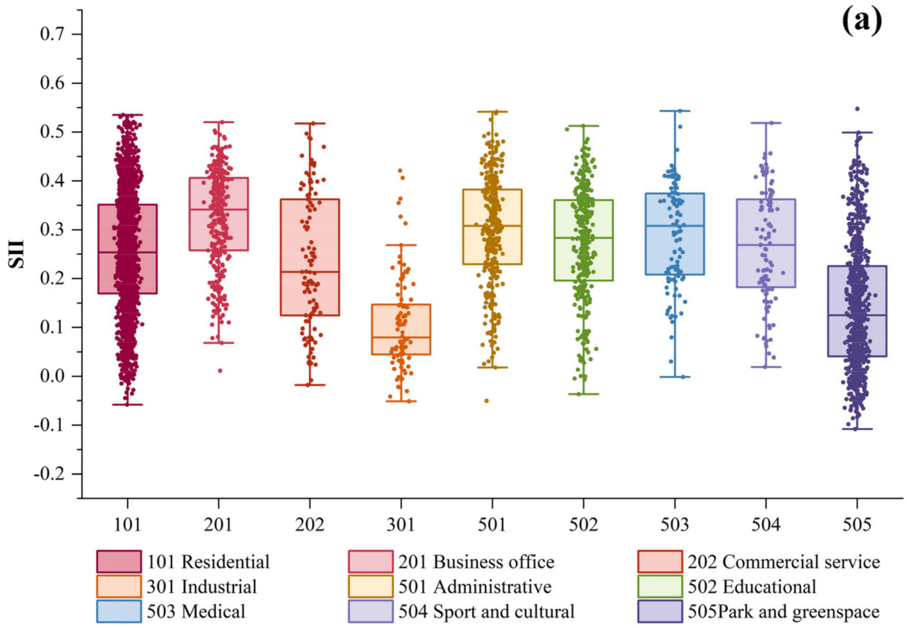

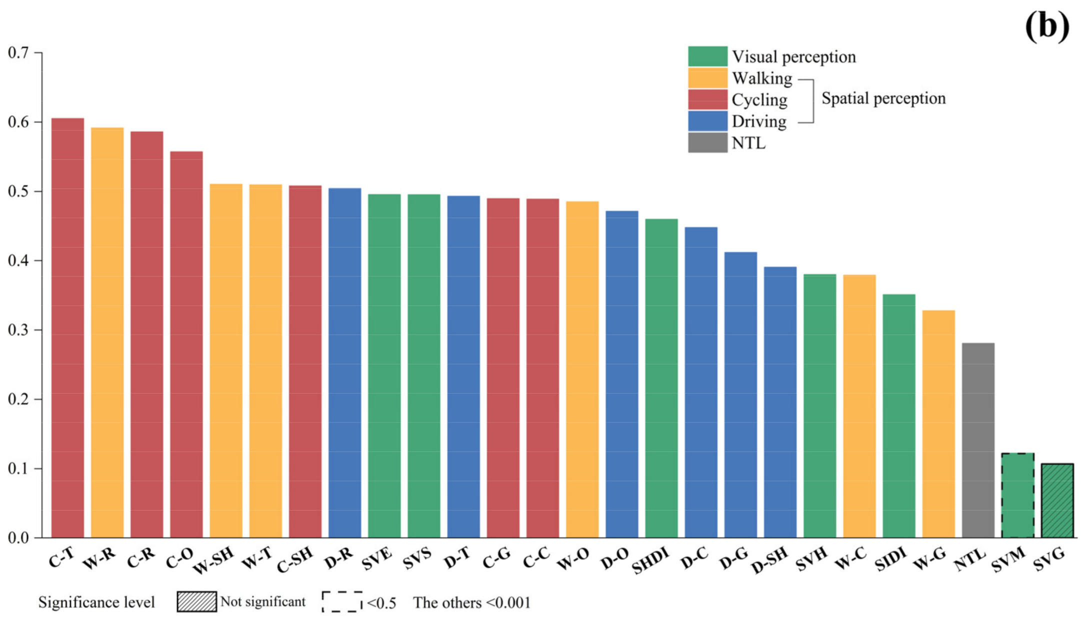

Figure 12. (**a**) Settlement intention index (SII) values of different land use categories, (**b**) influence of perception factors on the density of total population distribution (DTP), sorted from high to low.

To meet the growing population demand of the city, the urban land function is changing from the traditional single type to the mixed type [67,68]. Notably, the residential type classified by land use classification is no longer the only choice of population settlement [21,69]. As shown in Figure 12a, the SII value of residential land in the study area was widely distributed and portrayed no obvious aggregation. According to the SII calculation model, the residential areas having high SII values often portrayed higher environmental quality and better geographical locations. However, limited by their economic level, people will choose the most suitable residence within the affordable range [70]. Li et al. indicated that the spatial distribution of the accessibility of service facilities may shape the spatial distribution of apartment prices, which greatly affected the settlement choice of people having lower income [71]. Therefore, residential households with low SII values may be occupied by low-income populations; this conclusion can guide future studies on social equity and urban planning. In this study, the SII values of industrial areas were the lowest, which was consistent with peoples' negative attitude towards industrial areas, when choosing potential residential locations [72]. Notably, a few SII values for the office, commercial, medical, sports, and cultural land types were high, reflecting the tendency of these blocks to transform to mixed land use. The distribution of SII values for commercial land were scattered, related to the block types of large commercial areas and mixed commercial and residential areas. However, the main commercial areas with fewer residential buildings, such as Xidan, Wangfujing, and Sanlitun, portrayed low SII values, whereas the commercial plots with more residential buildings portrayed high SII values. However, the prevailing land use classification could not divide the types of parks and green land plots into commercial tourist attractions and leisure places near houses according to their functions, resulting in the mixed distribution of high and low SII values of parks and green land plots.

Therefore, the SII model constructed in this study portrayed the following application potential:

- Identification of population mobility in residential areas: the higher the SII value, the stronger the peoples' desire to live in the region for a long time, and people settled in residential areas having lower SII values may have the idea of migrating to areas with high SII values.
- Identification of mixed land use: the model provides a basis for the detailed study of land use categories and assists in the identification of mixed land use. In addition to residential areas, land use types having high SII values may include, or be close to, more residential buildings. This can also be used as one of the references to judge the mixing degree of land use in a particular area.

5.2.2. Comparison with Prevailing Population Distribution Studies

At present, the interdisciplinary studies on urban environment and population are generally based on the total population data in the census results. In addition to these results, compared to settled population, the total population also includes migrant workers, people visiting relatives, and other floating population. Using this information, we supplemented the factor detection analysis of the density of total population distribution (DTP) at the street scale. The results are shown in Figure 12b. For different travel modes, the accessibility to residential facilities in the three travel modes had high effects on the DTP. Compared with the other two travel modes, the driving accessibility to commercial facilities had a greater influence and the driving accessibility to science education and health facilities had a lower influence. For different types of facilities, among the three travel modes, the cycling accessibility various facilities had high influence. The driving accessibility to traffic, residential, office, and education and health facilities had the least influence on the DTP. The walking accessibility to commercial facilities, green spaces, and square facilities had the least influence on the DTP. Visual perception factors that had a significant influence on DTP are ranked as SVE, SVS, SHDI, SVH, SIDI according to their relative importance to DTP. Their interpretation rates to the spatial heterogeneity of DTP were higher than NTL. SVM and SVG have no significant influence on DTP.

Compared with Figure 7a, the influence of perception factors on the DTP was weaker than that on the DSP. Khraif indicated that urban environment may not be the most influential determinants for the floating population's choice of residential location [73]. Moreover, the influence of the SVE and SVS on the DTP was weaker than that on the DSP, while the influence of two diversity factors, namely, SHDI and SIDI, increased significantly. This indicated that, when choosing their residence, the floating population paid more attention to the diversity of urban functions, without considering the degree of motorization and greening. Among the spatial perception factors and all travel modes, the accessibility of the cycling travel mode to various facilities was not the most influential, and the accessibility of walking mode improved. The influence of driving accessibility was still low, which was consistent with Yan [54]. The difference in the influence of human perceived factors reflected the different factors considered by the two types of population when selecting their residence. Zhang indicated that the floating population was more likely to live in a relatively low-quality environment [74]. Therefore, the information reflected by the SII can provide a reliable reference for the refinement of population distribution types in the future.

5.3. Limitations

This study has the following limitations:

1. We focused on only the human perceptions of the physical characteristics of urban environment. Social and psychological characteristics, such as economic conditions, job attributes, and social relationships, are also important influencing factors, and thus, should be considered and analyzed in future studies [73,75].
2. To ensure the universality of the method, the data sources we used were available open-source data. Peoples' sense of smell [76–79] and hearing [80,81] with respect to the environment are proven to affect their behavior. Due to the limitations in data acquisition, we did not consider these factors in our study. Notably, whether these factors have a significant influence on peoples' living behavior remainss unconfirmed.
3. To simplify the construction of the SII model, we did not add the perception factors that had a low influence. Future studies need to further consider the interaction between different factors in the construction of SII.
4. In our study, it was difficult to ensure consistency in the acquisition time of SVIs. Notably, the urban landscape difference caused by time difference is an important error source of visual perception quantification of urban public space and must be addressed in future related studies.
5. Due to the limitation of spatial accuracy of DSP, our contributing factor analysis can only be carried out at the street scale. In addition, our validation of the effectiveness of SII is still insufficient due to the limitation of the temporal accuracy of the settled population distribution data.

6. Conclusions

Based on the measurement of human perceptions, in this study, we explored the relationship between urban-settled population and urban environment. We explained the effects of the characteristics of the human perception of urban environment on the distribution of settled population and determined the SII values of different areas at block scale, to predict the distribution trend of settled population. The main conclusions of this study are detailed below:

1. Human perception was one of the important factors influencing the distribution of urban-settled population. Almost all human perception factors had a significant influence on the distribution of settled population, and the influence varied with environmental factors and modes of travel. Visual perception factors related to the built environment and cycling accessibility to various facilities portrayed the greatest influence. Notably, human perception factors having low independent influence portrayed excellent explanatory power, when combined with other factors.
2. The population settled in Beijing is concentrated in the center of the city. Managers can improve the urban environmental construction around the fifth ring road by analyzing the mutual enhancement of perception factors, thus alleviating the uneven distribution of the settled population in the city.
3. A combination of the geographic detector method and AHP for the construction of the SII values is objective and practical. This combination method considers the differences in the effects of various human perception factors on the spatial distribution of settled population in different urban environments and can be extended to different cities.

The limitations of data and technology led to some limitations in the selection of human perceptual factors and the validity of research and analysis. In future research, we need to further improve the human perception system and consider how to take the interaction between factors into account in index construction. In addition, we will explore higher precision data sources and more accurate data processing methods to improve the rationality of the experiment. A mechanism exploration and adaptability analysis based on multiple city experiments is also needed.

The settled population and its density in the sustainable urban development indicator set are important indicators of social indicators. As an effective supplement to population distribution data, the results of this study can provide data support for the calculation of relevant indicators in SDG11. For example, SII can be used in SDG 11.3.1 (ratio of land consumption rate to population growth rate) as the urban-settled population growth rate. In addition, the results of this study can guide urban planners and managers to carry out targeted urban optimization construction and improve resource allocation from the view of the distribution of settled population, so as to ensure the sustainable development of cities.

The research on the distribution of settled population is still weak in the exploration of urban sustainability. Hope our research can provide new methods and ideas for scholars all over the world to study the distribution of settled population.

Author Contributions: Conceptualization, J.Q.; methodology, J.Q. and X.W.; software, J.Q.; validation, Q.M. and L.Z.; formal analysis, J.Q.; investigation, J.Q.; resources, Q.M.; data curation, L.Z.; writing—original draft preparation, J.Q.; writing—review and editing, X.W. and J.G.; visualization, J.Q.; supervision, Q.M.; project administration, Q.M., L.Z., L.J. and T.J.; funding acquisition, Q.M. All authors have read and agreed to the published version of the manuscript.

Funding: This work was financially supported by China National Natural Science Foundation; and the Bilateral Chinese-Hungarian Project: The research on the multi-perspective evaluation of urban green space based on remote sensing and street view data [Project number 42171357]; Investigation of the characteristics of surface shapes in rural environment based on point clouds and remote sensing data [Project number No. 2019-2.1.11-TÉT-2020-00171].

Data Availability Statement: Not applicable.

Conflicts of Interest: The authors declare that they have no known competing financial interests or personal relationships that could have appeared to influence the work reported in this paper.

References

1. United Nations, Department of Economic and Social Affairs. *World Urbanization Prospects: The 2008 Revision*; Department of Economic and Social Affairs: New York, NY, USA, 2009.
2. Aerni, P. Coping with Migration-Induced Urban Growth: Addressing the Blind Spot of UN Habitat. *Sustainability* **2016**, *8*, 800. [CrossRef]
3. Pourghasemi, H.R.; Gayen, A.; Panahi, M.; Rezaie, F.; Blaschke, T. Multi-Hazard Probability Assessment and Mapping in Iran. *Sci. Total Environ.* **2019**, *692*, 556–571. [CrossRef] [PubMed]
4. Chen, X.; Li, F.; Li, X.; Hu, Y.; Hu, P. Evaluating and Mapping Water Supply and Demand for Sustainable Urban Ecosystem Management in Shenzhen, China. *J. Clean. Prod.* **2020**, *251*, 119754. [CrossRef]
5. Lin, Y.; Chen, X.; Huang, L.; Zhu, C.; Shahtahmassebi, A.R.; Zhang, J.; Shen, S.; Peng, R.; Deng, J.; Wang, K.; et al. Fine-Scale Mapping of Urban Ecosystem Service Demand in a Metropolitan Context: A Population-Income-Environmental Perspective. *Sci. Total Environ.* **2021**, *781*, 146784. [CrossRef]
6. Feng, Z.; Li, F.; Yang, Y.; Li, P. The Past, Present, and Future of Population Geography in China: Progress, Challenges and Opportunities. *J. Geogr. Sci.* **2017**, *27*, 925–942. [CrossRef]
7. United Nations. *Transforming Our World: The 2030 Agenda for Sustainable Development*; United Nations: New York, NY, USA, 2015.
8. Wang, L.; Fan, H.; Wang, Y. Improving Population Mapping Using Luojia 1-01 Nighttime Light Image and Location-Based Social Media Data. *Sci. Total Environ.* **2020**, *730*, 139148. [CrossRef]
9. Jiang, S.; Zhang, Z.; Ren, H.; Wei, G.; Xu, M.; Liu, B. Spatiotemporal Characteristics of Urban Land Expansion and Population Growth in Africa from 2001 to 2019: Evidence from Population Density Data. *ISPRS Int. J. Geo-Inf.* **2021**, *10*, 584. [CrossRef]
10. Chen, Y.; Li, X.; Huang, K.; Luo, M.; Gao, M. High-Resolution Gridded Population Projections for China Under the Shared Socioeconomic Pathways. *Earths Future* **2020**, *8*, e2020EF001491. [CrossRef]
11. Xu, Y.; Song, Y.; Cai, J.; Zhu, H. Population Mapping in China with Tencent Social User and Remote Sensing Data. *Appl. Geogr.* **2021**, *130*, 102450. [CrossRef]
12. Zhao, X.; Zhou, Y.; Chen, W.; Li, X.; Li, X.; Li, D. Mapping Hourly Population Dynamics Using Remotely Sensed and Geospatial Data: A Case Study in Beijing, China. *GISci. Remote Sens.* **2021**, *58*, 717–732. [CrossRef]

13. Wardrop, N.A.; Jochem, W.C.; Bird, T.J.; Chamberlain, H.R.; Clarke, D.; Kerr, D.; Bengtsson, L.; Juran, S.; Seaman, V.; Tatem, A.J. Spatially Disaggregated Population Estimates in the Absence of National Population and Housing Census Data. *Proc. Natl. Acad. Sci. USA* **2018**, *115*, 3529–3537. [CrossRef] [PubMed]
14. Liu, L.; Silva, E.A.; Long, Y. Block-Level Changes in the Socio-Spatial Landscape in Beijing: Trends and Processes. *Urban Stud.* **2019**, *56*, 1198–1214. [CrossRef]
15. Liu, Q.; Tian, Y.; Yin, K.; Zhang, F.; Huang, H.; Chen, F. Landscape Pattern Theoretical Optimization of Urban Green Space Based on Ecosystem Service Supply and Demand. *ISPRS Int. J. Geo-Inf.* **2021**, *10*, 263. [CrossRef]
16. Li, X. Examining the Spatial Distribution and Temporal Change of the Green View Index in New York City Using Google Street View Images and Deep Learning. *Environ. Plan. B Urban Anal. City Sci.* **2021**, *48*, 2039–2054. [CrossRef]
17. Song, Y.; Long, Y.; Wu, P.; Wang, X. Are All Cities with Similar Urban Form or Not? Redefining Cities with Ubiquitous Points of Interest and Evaluating Them with Indicators at City and Block Levels in China. *Int. J. Geogr. Inf. Sci.* **2018**, *32*, 2447–2476. [CrossRef]
18. Owen, N.; Humpel, N.; Leslie, E.; Bauman, A.; Sallis, J.F. Understanding Environmental Influences on Walking: Review and Research Agenda. *Am. J. Prev. Med.* **2004**, *27*, 67–76. [CrossRef]
19. Humpel, N.; Owen, N.; Leslie, E. Environmental Factors Associated with Adults' Participation in Physical Activity. A Review. *Am. J. Prev. Med.* **2002**, *22*, 188–199. [CrossRef]
20. Guo, J.Y.; Bhat, C.R. Operationalizing the Concept of Neighborhood: Application to Residential Location Choice Analysis. *J. Transp. Geogr.* **2007**, *15*, 31–45. [CrossRef]
21. Habib, M.A.; Miller, E.J. Reference-Dependent Residential Location Choice Model within a Relocation Context. *Transp. Res. Rec.* **2009**, *2133*, 92–99. [CrossRef]
22. Lin, T.; Wang, D.; Guan, X. The Built Environment, Travel Attitude, and Travel Behavior: Residential Self-Selection or Residential Determination? *J. Transp. Geogr.* **2017**, *65*, 111–122. [CrossRef]
23. Masoumi, H.; Aslam, A.B.; Rana, I.A.; Ahmad, M.; Naeem, N. Relationship of Residential Location Choice with Commute Travels and Socioeconomics in the Small Towns of South Asia: The Case of Hafizabad, Pakistan. *Sustainability* **2022**, *14*, 3163. [CrossRef]
24. Meyer, W.B.; Turner, B.L. *Changes in Land Use and Land Cover: A Global Perspective*; Cambridge University Press: Cambridge, UK, 1994; Volume 4, ISBN 0521470854.
25. Ewing, R.; Handy, S.; Brownson, R.C.; Clemente, O.; Winston, E. Identifying and Measuring Urban Design Qualities Related to Walkability. *J. Phys. Act. Health* **2016**, *3*, S223–S240. [CrossRef] [PubMed]
26. Hu, D.; Meng, Q.; Zhang, L.; Zhang, Y. Spatial Quantitative Analysis of the Potential Driving Factors of Land Surface Temperature in Different "Centers" of Polycentric Cities: A Case Study in Tianjin, China. *Sci. Total Environ.* **2020**, *706*, 135244. [CrossRef] [PubMed]
27. Zhang, L.; Ye, Y.; Zeng, W.; Chiaradia, A. A Systematic Measurement of Street Quality through Multi-Sourced Urban Data: A Human-Oriented Analysis. *Int. J. Environ. Res. Public Health* **2019**, *16*, 1782. [CrossRef] [PubMed]
28. Hansen, W.G. How Accessibility Shapes Land Use. *J. Am. Plan. Assoc.* **1959**, *25*, 73–76. [CrossRef]
29. Gehrke, S.R.; Singleton, P.A.; Clifton, K.J. Understanding Stated Neighborhood Preferences: The Roles of Lifecycle Stage, Mobility Style, and Lifestyle Aspirations. *Travel. Behav. Soc.* **2019**, *17*, 62–71. [CrossRef]
30. Zondag, B.; de Bok, M.; Geurs, K.T.; Molenwijk, E. Accessibility Modeling and Evaluation: The TIGRIS XL Land-Use and Transport Interaction Model for the Netherlands. *Comput. Environ. Urban Syst.* **2015**, *49*, 115–125. [CrossRef]
31. Baraklianos, I.; Bouzouina, L.; Bonnel, P.; Aissaoui, H. Does the Accessibility Measure Influence the Results of Residential Location Choice Modelling? *Transportation* **2020**, *47*, 1147–1176. [CrossRef]
32. Kim, J.H.; Pagliara, F.; Preston, J. The Intention to Move and Residential Location Choice Behaviour. *Urban Stud.* **2005**, *42*, 1621–1636. [CrossRef]
33. Jang, S.; Yi, C. Imbalance between Local Commuting Accessibility and Residential Locations of Households by Income Class in the Seoul Metropolitan Area. *Cities* **2021**, *109*, 103011. [CrossRef]
34. Yiannakoulias, N.; Bland, W.; Svenson, L.W. Estimating the Effect of Turn Penalties and Traffic Congestion on Measuring Spatial Accessibility to Primary Health Care. *Appl. Geogr.* **2013**, *39*, 172–182. [CrossRef]
35. Geurs, K.T.; De Montis, A.; Reggiani, A. Recent Advances and Applications in Accessibility Modelling. *Comput. Environ. Urban Syst.* **2015**, *49*, 82–85. [CrossRef]
36. Geurs, K.T.; van Wee, B. Accessibility Evaluation of Land-Use and Transport Strategies: Review and Research Directions. *J. Transp. Geogr.* **2004**, *12*, 127–140. [CrossRef]
37. Van Wee, B. Accessible Accessibility Research Challenges. *J. Transp. Geogr.* **2016**, *51*, 9–16. [CrossRef]
38. Liu, Y.; Shen, J. Modelling Skilled and Less-Skilled Interregional Migrations in China, 2000–2005. *Popul. Space Place* **2017**, *23*, e2027. [CrossRef]
39. Gong, P.; Chen, B.; Li, X.; Liu, H.; Wang, J.; Bai, Y.; Chen, J.; Chen, X.; Fang, L.; Feng, S.; et al. Mapping Essential Urban Land Use Categories in China (EULUC-China): Preliminary Results for 2018. *Sci. Bull.* **2020**, *65*, 182–187. [CrossRef]
40. Tsai, V.J.D.; Chang, C. Three-dimensional Positioning from Google Street View Panoramas. *IET Image Process.* **2013**, *7*, 229–239. [CrossRef]
41. Yin, L.; Wang, Z. Measuring Visual Enclosure for Street Walkability: Using Machine Learning Algorithms and Google Street View Imagery. *Appl. Geogr.* **2016**, *76*, 147–153. [CrossRef]

42. Chen, L.-C.; Papandreou, G.; Schroff, F.; Adam, H. Rethinking Atrous Convolution for Semantic Image Segmentation. *arXiv* **2017**, arXiv:1706.05587.
43. Cordts, M.; Omran, M.; Ramos, S.; Rehfeld, T.; Enzweiler, M.; Benenson, R.; Franke, U.; Roth, S.; Schiele, B. The Cityscapes Dataset for Semantic Urban Scene Understanding. In Proceedings of the 2016 IEEE Conference on Computer Vision and Pattern Recognition (CVPR), Las Vegas, NV, USA, 27–30 June 2016; pp. 3213–3223. [CrossRef]
44. Shanghai Municipal People's Government. *Shanghai Master Plan 2016–2040 (Draft)*; Shanghai Municipal People's Government: Shanghai, China, 2016.
45. Tang, J.; Long, Y. Measuring Visual Quality of Street Space and Its Temporal Variation: Methodology and Its Application in the Hutong Area in Beijing. *Landsc. Urban Plan.* **2019**, *191*, 103436. [CrossRef]
46. Xia, Y.; Yabuki, N.; Fukuda, T. Development of a System for Assessing the Quality of Urban Street-Level Greenery Using Street View Images and Deep Learning. *Urban For. Urban Green.* **2021**, *59*, 126995. [CrossRef]
47. Ki, D.; Lee, S. Analyzing the Effects of Green View Index of Neighborhood Streets on Walking Time Using Google Street View and Deep Learning. *Landsc. Urban Plan.* **2021**, *205*, 103920. [CrossRef]
48. Asgarzadeh, M.; Koga, T.; Hirate, K.; Farvid, M.; Lusk, A. Investigating Oppressiveness and Spaciousness in Relation to Building, Trees, Sky and Ground Surface: A Study in Tokyo. *Landsc. Urban Plan.* **2014**, *131*, 36–41. [CrossRef]
49. Asgarzadeh, M.; Lusk, A.; Koga, T.; Hirate, K. Measuring Oppressiveness of Streetscapes. *Landsc. Urban Plan.* **2012**, *107*, 1–11. [CrossRef]
50. McGarigal, K.; Cushman, S.A.; Neel, M.C.; Ene, E. FRAGSTATS: Spatial Pattern Analysis Program for Categorical Maps. Available online: https://www.umass.edu/landeco/research/fragstats/fragstats.html (accessed on 12 October 2009).
51. Li, J.; Li, J.; Yuan, Y.; Li, G. Spatiotemporal Distribution Characteristics and Mechanism Analysis of Urban Population Density: A Case of Xi'an, Shaanxi, China. *Cities* **2019**, *86*, 62–70. [CrossRef]
52. Liu, Y.; Zhang, Y.; Jin, S.T.; Liu, Y. Spatial Pattern of Leisure Activities among Residents in Beijing, China: Exploring the Impacts of Urban Environment. *Sustain. Cities Soc.* **2020**, *52*, 101806. [CrossRef]
53. Bittencourt, T.A.; Giannotti, M. The Unequal Impacts of Time, Cost and Transfer Accessibility on Cities, Classes and Races. *Cities* **2021**, *116*, 103257. [CrossRef]
54. Yan, X. Evaluating Household Residential Preferences for Walkability and Accessibility across Three U.S. Regions. *Transp. Res. Part D Transp. Environ.* **2020**, *80*, 102255. [CrossRef]
55. Song, Y.; Wang, J.; Ge, Y.; Xu, C. An Optimal Parameters-Based Geographical Detector Model Enhances Geographic Characteristics of Explanatory Variables for Spatial Heterogeneity Analysis: Cases with Different Types of Spatial Data. *GISci. Remote Sens.* **2020**, *57*, 593–610. [CrossRef]
56. Wang, X.; Meng, Q.; Zhang, L.; Hu, D. Evaluation of Urban Green Space in Terms of Thermal Environmental Benefits Using Geographical Detector Analysis. *Int. J. Appl. Earth Obs. Geoinf.* **2021**, *105*, 102610. [CrossRef]
57. Hu, D.; Meng, Q.; Schlink, U.; Hertel, D.; Liu, W.; Zhao, M.; Guo, F. How Do Urban Morphological Blocks Shape Spatial Patterns of Land Surface Temperature over Different Seasons? A Multifactorial Driving Analysis of Beijing, China. *Int. J. Appl. Earth Obs. Geoinf.* **2022**, *106*, 102648. [CrossRef]
58. Saaty, T.L.; Kearns, K.P. *The Analytic Hierarchy Process*; McGraw-Hill: New York, NY, USA, 1985.
59. Saaty, T.L. A Scaling Method for Priorities in Hierarchical Structures. *J. Math. Psychol.* **1977**, *15*, 234–281. [CrossRef]
60. Leake, C.; Malczewski, J. *GIS and Multicriteria Decision Analysis*; Wiley: New York, NY, USA, 2000; Volume 51.
61. Xue, R.; Wang, C.; Liu, M.; Zhang, D.; Li, K.; Li, N. A New Method for Soil Health Assessment Based on Analytic Hierarchy Process and Meta-Analysis. *Sci. Total Environ.* **2019**, *650*, 2771–2777. [CrossRef] [PubMed]
62. Lyu, H.M.; Sun, W.J.; Shen, S.L.; Arulrajah, A. Flood Risk Assessment in Metro Systems of Mega-Cities Using a GIS-Based Modeling Approach. *Sci. Total Environ.* **2018**, *626*, 1012–1025. [CrossRef] [PubMed]
63. Guo, B.; Zang, W.; Yang, X.; Huang, X.; Zhang, R.; Wu, H.; Yang, L.; Wang, Z.; Sun, G.; Zhang, Y. Improved Evaluation Method of the Soil Wind Erosion Intensity Based on the Cloud–AHP Model under the Stress of Global Climate Change. *Sci. Total Environ.* **2020**, *746*, 141271. [CrossRef]
64. Mokarram, M.; Pourghasemi, H.R.; Hu, M.; Zhang, H. Determining and Forecasting Drought Susceptibility in Southwestern Iran Using Multi-Criteria Decision-Making (MCDM) Coupled with CA-Markov Model. *Sci. Total Environ.* **2021**, *781*, 146703. [CrossRef]
65. Camara, M.; Jamil, N.R.; Abdullah, A.F.B.; Hashim, R.B.; Aliyu, A.G. Economic and Efficiency Based Optimisation of Water Quality Monitoring Network for Land Use Impact Assessment. *Sci. Total Environ.* **2020**, *737*, 139800. [CrossRef]
66. Bennett, M.M.; Smith, L.C. Advances in Using Multitemporal Night-Time Lights Satellite Imagery to Detect, Estimate, and Monitor Socioeconomic Dynamics. *Remote Sens. Environ.* **2017**, *192*, 176–197. [CrossRef]
67. Gong, Z.; Ma, Q.; Kan, C.; Qi, Q. Classifying Street Spaces with Street View Images for a Spatial Indicator of Urban Functions. *Sustainability* **2019**, *11*, 6424. [CrossRef]
68. Geist, C.; McManus, P.A. Geographical Mobility over the Life Course: Motivations and Implications. *Popul. Space Place* **2008**, *14*, 283–303. [CrossRef]
69. Lange, E. Our Shared Landscape: Design, Planning and Management of Multifunctional Landscapes. *J. Environ. Manag.* **2008**, *89*, 143–145. [CrossRef] [PubMed]

70. Lovell, S.T.; Johnston, D.M. Creating Multifunctional Landscapes: How Can the Field of Ecology Inform the Design of the Landscape? *Front. Ecol. Environ.* **2009**, *7*, 212–220. [CrossRef]
71. Waddell, P. Reconciling Household Residential Location Choices and Neighborhood Dynamics. *Sociol. Methods Res.* **2006**, 1–23.
72. Zhou, B.; Kockelman, K.M. Microsimulation of Residential Land Development and Household Location Choices: Bidding for Land in Austin, Texas. *Transp. Res. Rec.* **2008**, *2077*, 106–112. [CrossRef]
73. Li, H.; Wei, Y.D.; Wu, Y.; Tian, G. Analyzing Housing Prices in Shanghai with Open Data: Amenity, Accessibility and Urban Structure. *Cities* **2019**, *91*, 165–179. [CrossRef]
74. Weisbrod, G.E.; Lerman, S.R.; Ben-Akiva, M. Tradeoffs in Residential Location Decisions: Transportation versus Other Factors. *Transp. Policy Decis. Mak.* **1980**, *1*, 13–26.
75. Khraif, R.M. Permanent versus Temporary Rural Migrants in Riyadh, Saudi Arabia—A Logit Analysis of Their Intentions of Future Mobility. *GeoJournal* **1992**, *26*, 363–370. [CrossRef]
76. Zhang, Y. Unequal Living Conditions between Urban Migrants and Local Residents in China. *Procedia Eng.* **2017**, *198*, 728–735. [CrossRef]
77. Tang, S.; Feng, J. Understanding the Settlement Intentions of the Floating Population in the Cities of Jiangsu Province, China. *Asian Pac. Migr. J.* **2012**, *21*, 509–532. [CrossRef]
78. Easteal, M.; Bannister, S.; Kang, J.; Aletta, F.; Lavia, L.; Witchel, H. Urban Sound Planning in Brighton and Hove. In Proceedings of the Forum Acusticum, Krakow, Poland, 7–12 September 2014; pp. 7–12.
79. Henshaw, V. Urban Smellscapes: Understanding and Designing City Smell Environments. In *Urban Smellscapes*; Routledge: New York, NY, USA, 2013; pp. 1–256.
80. Lepore, F.; Kostara-Konstantinou, E.; Aletta, F.; Astolfi, A.; Kang, J. A Preliminary Investigation about the Influence of Soundscapes on People's Behaviour in an Open Public Space. In Proceedings of the 45th International Congress and Exposition on Noise Control Engineering, Hamburg, Germany, 21–24 August 2016; Volume 6, pp. 5219–5224.
81. Pheasant, R.; Horoshenkov, K.; Watts, G.; Barrett, B. The Acoustic and Visual Factors Influencing the Construction of Tranquil Space in Urban and Rural Environments Tranquil Spaces-Quiet Places? *J. Acoust. Soc. Am.* **2008**, *123*, 1446–1457. [CrossRef]